Int. J. Environ. Sci. Technol. (2017) 14:1635–1642
DOI 10.1007/s13762-017-1261-y

ORIGINAL PAPER

# In situ formation of AgNPs on *S. cerevisiae* surface as bionanocomposites for bacteria killing and heavy metal removal

**Z. Chen[1,2] · Z. Li[1] · G. Chen[1] · J. Zhu[3] · Q. Liu[3] · T. Feng[1]**

Received: 9 May 2016 / Revised: 17 November 2016 / Accepted: 30 January 2017 / Published online: 8 February 2017


**Abstract** Novel bionanocomposites, *S. cerevisiae*–AgNPs, were synthesized by in situ formation of AgNPs on *S. cerevisiae* surface using fulvic acids as reductants under simulated sunlight. *S. cerevisiae*–AgNPs were characterized using UV–Vis spectroscopy, scanning electron microscope, transmission electron microscope and Fourier transform infrared spectroscopy. These analyses showed that AgNPs were distributed on the surface of *S. cerevisiae*. The application of *S. cerevisiae*–AgNPs in bacteria killing and heavy metal removal was studied. *S. cerevisiae*–AgNPs effectively inhibited the growth of *E. coli* with increasing concentrations of *S. cerevisiae*–AgNPs. *E. coli* was killed completely at high concentration *S. cerevisiae*–AgNPs (e.g., 100 or 200 μg $mL^{-1}$). *S. cerevisiae*–AgNPs as excellent heavy metal absorbents also have been studied. Using $Cd^{2+}$ as model heavy metal, batch experiments confirmed that the adsorption behavior fitted the Langmuir adsorption isotherms and the $Cd^{2+}$ adsorption capacity of *S. cerevisiae*–AgNPs was 15.01 mg $g^{-1}$. According to adsorption data, the kinetics of $Cd^{2+}$ uptake by *S. cerevisiae*–AgNPs followed pseudo second-order kinetic model. Moreover, *S. cerevisiae*–AgNPs possessed ability of different heavy metals' removal (e.g., $Cr^{5+}$, $As^{5+}$, $Pb^{2+}$, $Cu^{2+}$, $Mn^{2+}$, $Zn^{2+}$, $Hg^{2+}$, $Ni^{2+}$). The simulated contaminated water containing *E. coli*, $Cd^{2+}$ and $Pb^{2+}$ was treated using *S. cerevisiae*–AgNPs. The results indicated that the bionanocomposites can be used to develop antibacterial agents and bioremediation agents for water treatment.

**Keywords** *S. cerevisiae*–AgNPs · Bacteria killing · Heavy metal removal · Water treatment

Editorial responsibility: Josef Trögl.

**Electronic supplementary material** The online version of this article (doi:10.1007/s13762-017-1261-y) contains supplementary material, which is available to authorized users.

✉ Z. Chen
chengroup_science@163.com

[1] Hunan Province Key Laboratory of Coal Resources Clean-Utilization and Mine Environment Protection, Hunan University of Science and Technology, Xiangtan 411201, Hunan, China

[2] College of Chemistry and Chemical Engineering, Hunan University, Changsha 410082, Hunan, China

[3] College of Architecture and Urban Planning, Hunan University of Science and Technology, Xiangtan 411201, Hunan, China

## Introduction

Water pollution has been regarded as a global environmental problem with harmful effect on human health and ecological safety. Heavy metals and microbial contaminants make the problem more and more serious (Fawell and Nieuwenhuijsen 2003). To avoid pollution damages from these contaminants, it is critical to kill bacteria and remove heavy metal from water (Nancharaiah et al. 2015). Adsorption as an alternative process in water treatment has the characteristics of simplicity, rapidness, high efficiency and low cost (Ali and Gupta 2007; Ali et al. 2012; Ali 2014). Different adsorbents including active carbon, nanosized metal oxide materials have been used for pollutants removal from water (Ali et al. 2016a, b, c; Ali 2010, 2012). Biosorption using biological materials as adsorbents has also been considered as a perfect method for the removal of the low concentration of pollutant from water (Hansda et al. 2016; Li and Tao 2015). Microorganisms as a biological adsorbent have a good adsorption

for heavy metal (Javanbakht et al. 2014). Different types of microorganisms such as bacteria and yeast can be used to remove heavy metal with the advantages of simple preparation, low cost and environment friendliness (Li et al. 2013; Barboza et al. 2015).

Silver nanomaterials with broad-spectrum antimicrobial activity have been widely applied in water disinfection and microbial control (Loo et al. 2013; Lin et al. 2013). Though many chemical and physical methods could be used to prepare silver nanomaterials, these synthesis methods were characterized by high energy consumption, low efficiency and secondary pollution (Zhang et al. 2016). Recently, biosynthesis of silver nanomaterials has been developed as a low-cost, convenient, efficient and environmentally friendly method (Salunke et al. 2016; Velusamy et al. 2016; Ahmad et al. 2016). Microorganisms as nanomaterials biosynthesis factories have the potential to prepare silver nanomaterials. Moreover, the synthesized bionanocomposites can be used to remove pollutants such as pesticide and bacteria due to the adsorption property of microorganisms and the antibacterial property of silver nanomaterials (Das et al. 2012). Microbial cell, microbial extract or microbial extracellular polymeric substances can be used to reduce $Ag^+$-silver nanomaterials (Park et al. 2016). But, there are some disadvantages in a typical microbial biosynthesis of silver nanomaterials. For example, it is difficult to screen silver tolerant microbe with characteristic of silver nanomaterials synthesis (Salunkhe et al. 2011). Obtaining microbial extract or extracellular polymeric substances as reductants for silver nanomaterials preparation is complex and laborious (Wei et al. 2012). So it is necessary to develop a new method for silver bionanocomposites synthesis to remove heavy metal and bacteria.

In the manuscript, a simple, rapid, eco-friendly method for silver bionanocomposites preparation has been described. When $Ag^+$ was adsorbed on *S. cerevisiae* surface, in situ reduction of $Ag^+$ to AgNPs on *S. cerevisiae* surface was performed by fulvic acids as reductants under simulated sunlight (Scheme S1). At the same time, *S. cerevisiae* was used as biosorbent for heavy metal removal. *S. cerevisiae*–AgNPs possessed the characteristic of antibacterial effect and kept the ability of heavy metal removal.

The synthesis of *S. cerevisiae*–AgNPs was performed at Hunan University of Science and Technology between January and August 2015. *S. cerevisiae*–AgNPs were characterized at Hunan University between January and August 2015. The antimicrobial and adsorption experiments were performed at Hunan University and Hunan University of Science and Technology in 2015–2016.

## Materials and methods

### Materials

Chemical reagents including $K_2Cr_2O_7$, $Na_3AsO_4$, $Pb(NO_3)_2$, $Cu(NO_3)_2$, $HgCl_2$, $CdCl_2$, $MnSO_4$, $NiSO_4$, $ZnSO_4$ and biological reagents were purchased from China National Pharmaceutical Group Corporation. *S. cerevisiae* was purchased from the local supermarket. *E. coli* was a preserved strain in our laboratory.

### Instruments

The characteristics of *S. cerevisiae*–AgNPs were analyzed by Varian Cary300 UV–Vis spectrophotometer, Fourier transform infrared Nicolet 5700 spectrophotometer, field emission scanning electron microscope (FESEM, Model S-4800) and transmission electron microscope (JEM 3010) equipped with an energy-dispersive X-ray spectroscopic analysis (EDXA). Hg and As were measured using Agilent 200 Series AA atomic absorption spectrometer equipped with a VGA 77 AA hydride generator. Other heavy metals were measured using Hitachi Z-2000 atomic absorption spectrometer.

### *S. cerevisiae*–AgNPs preparation

*S. cerevisiae* was transferred into YPD culture medium and shaken overnight at 30 °C. One hundred milliliters of *S. cerevisiae* culture was centrifuged at 4000 rpm and washed three times to collect cell. After 30-s vigorous vortex reaction, 100 mL of resuspended *S. cerevisiae* containing 2 mM $AgNO_3$ was transferred into a beaker for 5 min stirring constantly. 0.1 g $L^{-1}$ fulvic acid was added for another 5-min stirring constantly. The solution was exposed for 5 min under a CHF-XM500 xenon lamp with a parallel light source system. Centrifugation at 4000 rpm, the precipitate was collected. And the collected *S. cerevisiae*–AgNPs were washed three times to remove free AgNPs. *S. cerevisiae*–AgNPs were freeze-dried overnight and kept at 4 °C.

### Bacteria killing

*Escherichia coli* was grown in LB broth and incubated on orbital shaker at 37 °C. The growth rate and concentration of *E. coli* were determined by measuring optical densities (OD) at 600 nm using UV–Vis spectrophotometer (Sreeprasad et al. 2011).

One milliliter of *E. coli* ($OD_{600}$ = 1.51) was transferred into 150 mL LB medium containing different doses of *S. cerevisiae*–AgNPs (0, 5, 10, 20, 30, 40, 50, 60, 70, 80, 90,

100 μg $mL^{-1}$). At a certain time interval, 1 mL of *E. coli* suspension was measured at $OD_{600}$ after three times dilution using sterile water.

One milliliter of *E. coli* ($OD_{600}$ = 1.86) was harvested by centrifugation at 4000 rpm. The collected cell was washed and resuspended using sterile water. Different doses of *S. cerevisiae*–AgNPs (0, 20, 40, 50, 100, 200 μg $mL^{-1}$) were added. After 2-h cultivation at 37 °C, *E. coli* soup was diluted $10^5$ times. One hundred microliters of *E. coli* diluent was spreaded and cultivated on LB plates (LB broth with 1.5% agar) at 37 °C for 24 h. *E. coli* colonies were counted using the colony-forming units (CFU) counting method (Wang et al. 2013). Each sample was carried out in triplicate. Photographs were recorded by Canon digital camera.

### Heavy metal removal

Heavy metal adsorption experiments were performed using $Cd^{2+}$ as model heavy metal in 50-mL flasks containing 2 mg $mL^{-1}$ *S. cerevisiae*–AgNPs at 150 rpm. The effect of pH on $Cd^{2+}$ adsorption was investigated at 20 m $L^{-1}$ $Cd^{2+}$ under different pHs varying from 4 to 6. The effect of reaction time on $Cd^{2+}$ adsorption was studied at different initial $Cd^{2+}$ concentrations from 10 to 80 mg $L^{-1}$. Varied concentrations from 5 to 80 mg $L^{-1}$ $Cd^{2+}$ adsorption were explored to study adsorption isotherms.

### Application of *S. cerevisiae*–AgNPs on simulated wastewater

After 6 h reaction using 2 mg $mL^{-1}$ *S. cerevisiae*-AgNPs, 20 mg $L^{-1}$$Pb^{2+}$, $Mn^{2+}$, $Zn^{2+}$, $Ni^{2+}$, $Hg^{2+}$, $Cu^{2+}$, $As^{5+}$ or $Cr^{6+}$ was detected. Simulated wastewater was prepared by adding heavy metals (10 mg $L^{-1}$ $Pb^{2+}$ and 10 mg $L^{-1}$ $Cd^{2+}$) and *E. coli* ($\approx 4.71 \times 10^7$) to the filtered Xiangjiang river water. Heavy metals and *E. coli* in the simulated wastewater were treated using 2 mg $mL^{-1}$ *S. cerevisiae*–AgNPs.

## Results and discussion

### Formation and characterization of *S. cerevisiae*–AgNPs

Biosorption is highly desirable for control of heavy metal pollution in water. *S. cerevisiae* has been used for heavy metal biosorption due to its advantages in high uptake, wide distribution, low cost and easy cultivation (Wang and Chen 2006). Moreover, the active groups of *S. cerevisiae* surface, such as hydroxyl group and carboxylic acid group, can act as binding site and nucleation site for AgNPs (Chen et al. 2014). $Ag^+$ is adsorbed on the surface of *S. cerevisiae*, and the adsorbed $Ag^+$ cannot form AgNPs in a short time (Korbekandi et al. 2016). Under simulated sunlight, $Ag^+$ can form AgNPs by spontaneous reduction of silver facilitated by carboxylic acid groups from peptidoglycan (Nam et al. 2008), but the process takes several days. In the experiment, fulvic acids act as environmentally safe reductants to accelerate the reduction of $Ag^+$–AgNPs under simulated sunlight (Yin et al. 2012).

The color of *S. cerevisiae* was changed from white to orange yellow within several minutes. The color change indicated that AgNPs were synthesized on *S. cerevisiae* surface. The UV–Vis spectra of *S. cerevisiae*–AgNPs exhibited an ultraviolet absorption peak at about 417 nm due to surface plasmon resonance of AgNPs (Fig. S1). The photographs of *S. cerevisiae*–AgNPs or AgNPs before and after centrifugation showed that free AgNPs cannot be centrifuged at speed of 4000 rpm, but AgNPs can be centrifuged by binding to *S. cerevisiae* (Fig. S2). SEM image indicated that a large number of AgNPs were distributed on *S. cerevisiae* surface (Fig. 1b). TEM micrograph further confirmed that AgNPs were synthesized (Fig. 1a). High-resolution TEM (HRTEM) image showed that crystalline AgNPs with the lattice distance of 0.233 nm were obtained (Yin et al. 2012; Das et al. 2013) (Fig. 1c). A characteristic peak of silver was about 3.0 keV from EDS spectrum (Fig. 1d).

By comparing the FTIR spectra of pristine *S. cerevisiae* and *S. cerevisiae*–AgNPs, the chief compositions and structure of *S. cerevisiae* remained intact (Fig. 2) (Naumann 2006; Das et al. 2012; Selvakumar et al. 2011). The broad spectral feature of 3313 $cm^{-1}$ resulted from N–H and O–H stretching vibration modes. The absorbance band at 1652.1 $cm^{-1}$ was attributed to the C=O stretching of amide I. The combination of N–H bending mode and C–N stretch vibration mode in amide II was response to 1541.3 $cm^{-1}$ frequency. A weak band at 1398.1 $cm^{-1}$ was related to the symmetrical stretching vibration of C=O in $COO^-$ functional groups of amino acid. The bands near 1241.8 and 1077.7 $cm^{-1}$ represented amide III band components of proteins and phosphate group of lipoprotein or phospholipids, respectively. The FTIR spectrum changes of *S. cerevisiae*–AgNPs were observed. The shift from 3313 to 3392.6 $cm^{-1}$ and the appearance of a broadening new band at 3392.6 $cm^{-1}$ indicated that part of hydroxyl groups involved into AgNPs formation (Chen et al. 2014). The changes of amide I and amide II absorbance band may be a result of the roles of amide linkages in AgNPs formation (Das et al. 2012). The conversion of $COO^-$ groups from 1398.1 to 1395.2 $cm^{-1}$ showed that the ionized carboxyl groups play important role in the formation of AgNPs (Chen et al. 2014; Selvakumar et al. 2011). The

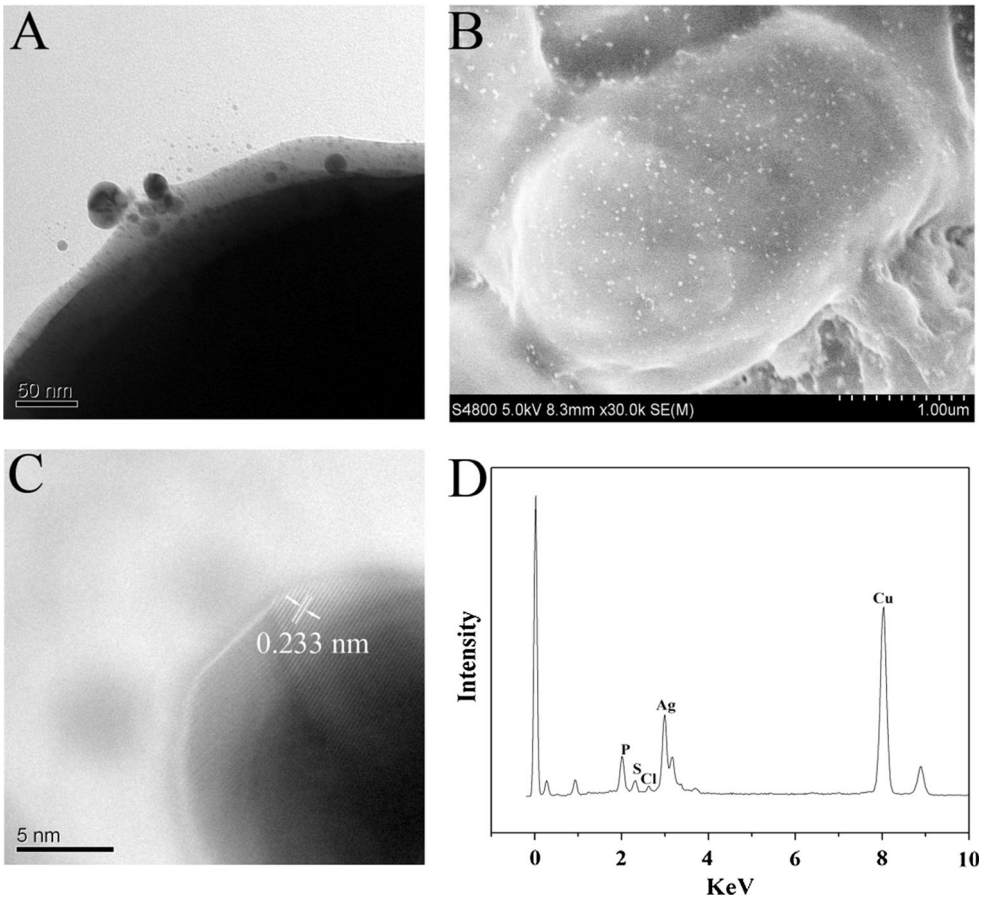


**Fig. 1** TEM image (**a**), SEM image (**b**), HRTEM image (**c**), EDX spectrum (**d**) of *S. cerevisiae*–AgNPs

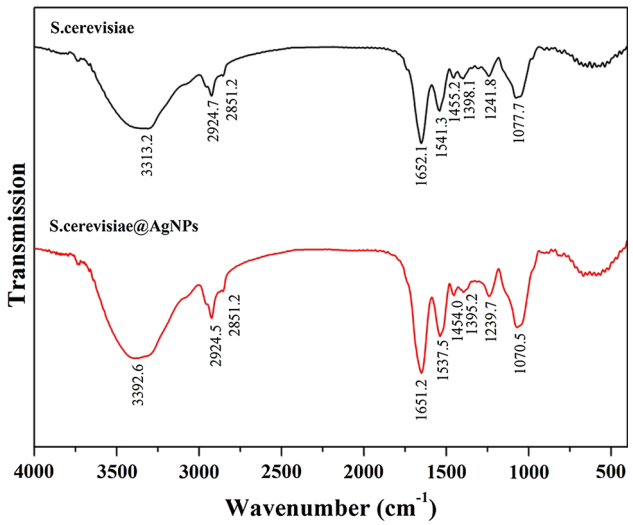


**Fig. 2** FTIR spectra of *S. cerevisiae* and *S. cerevisiae*–AgNPs

shift of band at 1077.7 $cm^{-1}$ implied that the stability of AgNPs was mediated by the phosphate group of lipoprotein (Das et al. 2012).

## Antimicrobial activity of *S. cerevisiae*–AgNPs

In liquid culture, *E. coli* growth kinetics was monitored to evaluate antimicrobial activity of *S. cerevisiae*–AgNPs. A growth delay of *E. coli* was observed with increasing *S. cerevisiae*–AgNPs concentrations (Fig. 3a). 5 μg $mL^{-1}$ of *S. cerevisiae*–AgNPs caused a growth delay. At dose of 60 μg $mL^{-1}$, *E. coli* proliferated very slowly. *E. coli* was inhibited completely when *S. cerevisiae*–AgNPs concentration exceed 70 μg $mL^{-1}$. Figure 3b shows the number of *E. coli* colonies on LB agar plates under different concentrations of *S. cerevisiae*–AgNPs. A vast array of *E. coli* colonies was observed in the absence of *S. cerevisiae*–AgNPs. The number of *E. coli* colonies was remarkably reduced under 40 or 50 μg $mL^{-1}$ *S. cerevisiae*–AgNPs. 100% inhibition was achieved in the presence of 100 or 200 μg $mL^{-1}$. Results indicated that *S. cerevisiae*–AgNPs could significantly restrain bacteria growth. The antibacterial property of *S. cerevisiae*–AgNPs is due to the large amounts of the toxic effect of AgNPs on *S. cerevisiae* surface.

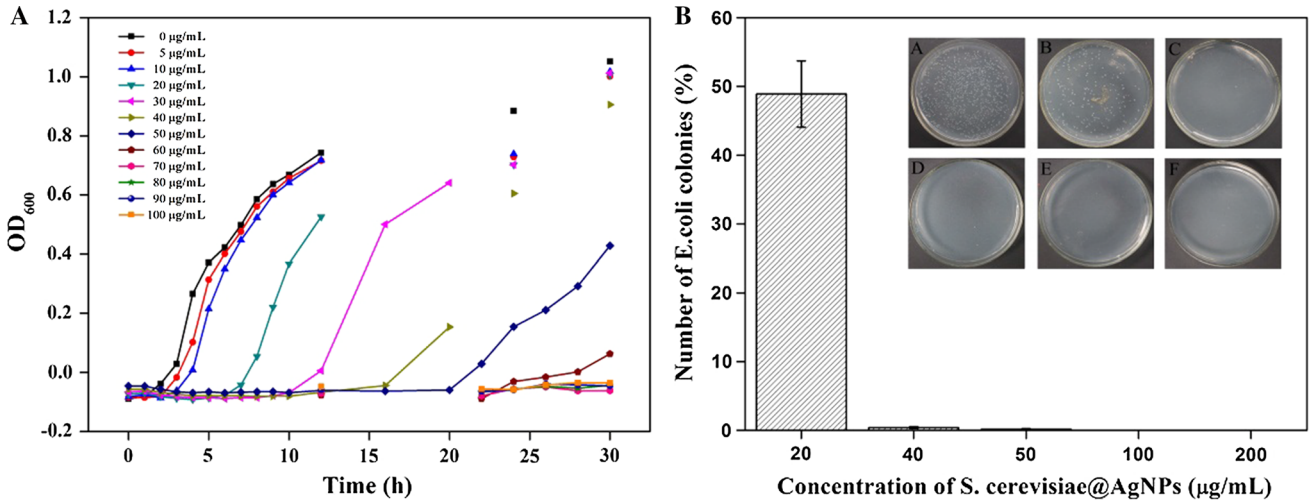


**Fig. 3** **a** Growth of *E. coli* in LB medium containing different concentrations of *S. cerevisiae*–AgNPs. **b** The number of *E. coli* colonies in the presence of different concentrations of *S. cerevisiae*–AgNPs as a percentage of the number of *E. coli* colonies in the absence of *S. cerevisiae*–AgNPs. *Inset* the photographs under different concentrations of *S. cerevisiae*–AgNPs. **A** 0 μg $mL^{-1}$, **B** 20 μg $mL^{-1}$, **C** 40 μg $mL^{-1}$, **D** 50 μg $mL^{-1}$, **E** 100 μg $mL^{-1}$, **F** 200 μg $mL^{-1}$

## Heavy metal biosorption of *S. cerevisiae*–AgNPs

Cadmium is a common kind of heavy metal that is most harmful to environment and human health (Clares et al. 2015). $Cd^{2+}$ was chosen as model heavy metal to study heavy metal biosorption in the study. The influences of pH on $Cd^{2+}$ removal were studied in Fig. S3. With the increase in pH value, removal efficiency was gradually improved. Higher adsorption at pH 6 could be due to the stronger electrostatic attraction between the negatively charged cell surface and the positively charged $Cd^{2+}$.

The effects of contact time on $Cd^{2+}$ adsorption were investigated (Fig. S4). The adsorption was very fast in the first few minutes, followed closely by the slow adsorption. The kinetics of $Cd^{2+}$ uptake showed that the adsorption can be divided into two processes: the rapid beginning followed by the slow phase. The pseudo second-order kinetic model was used to study $Cd^{2+}$ adsorption kinetics (Table 1). The calculated $q_e$ values were proved to be close to the experimental $q_e$ values. The correlation coefficient values ($R^2$) were close to 1. As shown in Fig. 4, the adsorption kinetics of $Cd^{2+}$ can be well described by pseudo second-order kinetic model based on the assumption that the rate-limiting step may be chemical adsorption involving valence forces through sharing or exchange of electrons (Belala et al. 2011; Chen and Wang 2010).

**Table 1** Parameters of pseudo second-order kinetic model for $Cd^{2+}$ adsorption on *S. cerevisiae*–AgNPs

| The pseudo second-order kinetic model | | | | |
|---|---|---|---|---|
| Cd concentration (mg $L^{-1}$) | 10 | 20 | 40 | 80 |
| $q_e$ (exp) (mg $g^{-1}$) | 4.375 | 7.25 | 11.25 | 13 |
| $q_e$ (cal) (mg $g^{-1}$) | 4.16 | 7.37 | 11.31 | 13.57 |
| $K_2$ (g $mg^{-1}$ $min^{-1}$) | 0.6353 | 0.3935 | 0.5414 | 0.2046 |
| $R^2$ | 0.9995 | 0.9997 | 0.9981 | 0.9992 |

The pseudo second-order kinetic model: $t/q_t = 1/k_2 q_e^2 + t/q_e$, where $q_t$ (mg $g^{-1}$) and $q_e$ (mg $g^{-1}$) represent the adsorption capacity at the equilibrium and time $t$, respectively, and $k_2$ (g $mg^{-1}$ $min^{-1}$) represents the rate constant of the pseudo second-order kinetic model

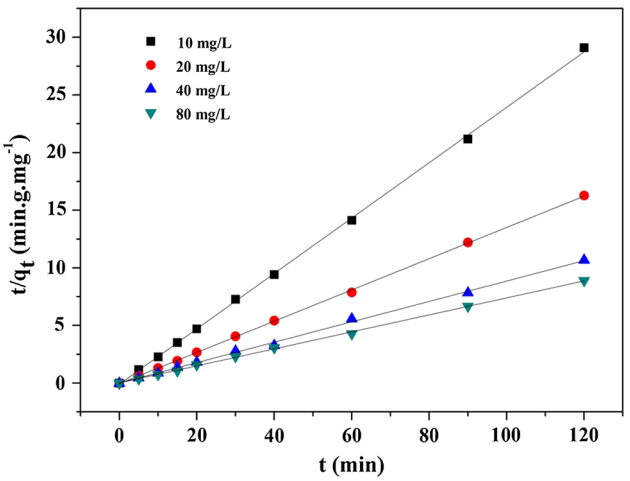


**Fig. 4** Second-order adsorption kinetics of different concentrations of $Cd^{2+}$

Langmuir model and Freundlich model were described to simulate $Cd^{2+}$ adsorption (Wang and Chen 2006; Ali et al. 2016c). Langmuir isotherm model presented a better fit to depict $Cd^{2+}$ uptake on *S. cerevisiae*–AgNPs, as shown in Fig. 5, and the results showed that *S. cerevisiae* binding to AgNPs does not lose the removal ability of adsorbent for heavy metal and monolayer adsorption takes place on *S. cerevisiae*–AgNPs surface (Selvakumar et al.

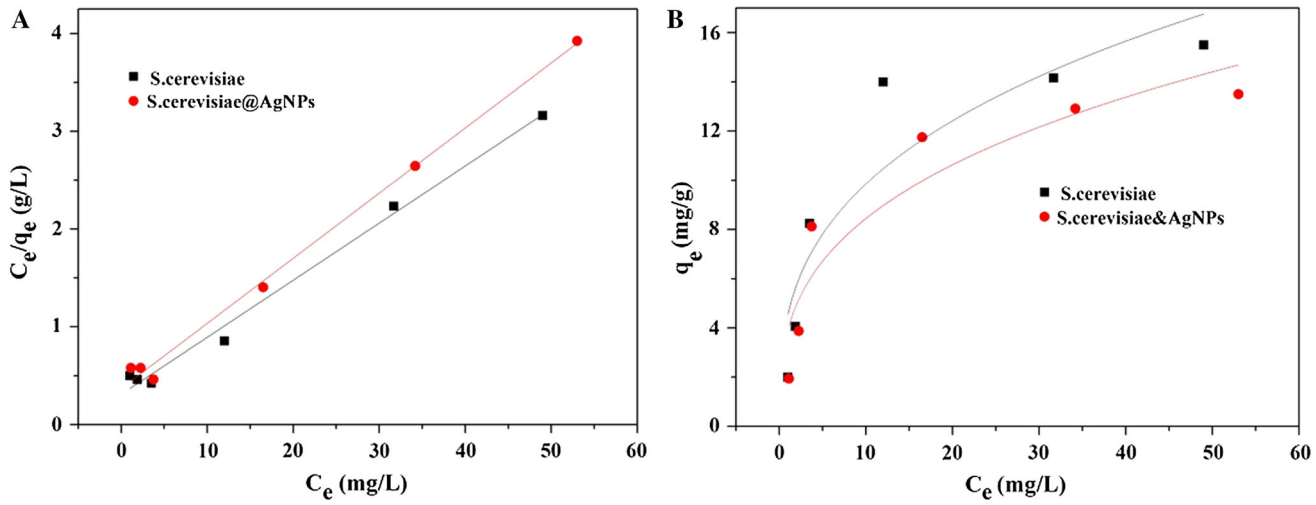


**Fig. 5** **a** Langmuir and **b** Freundlich isotherm model for $Cd^{2+}$ adsorption on *S. cerevisiae* or *S. cerevisiae*–AgNPs

**Table 2** Parameters of Langmuir and Freundlich for $Cd^{2+}$ adsorption on *S. cerevisiae* or *S. cerevisiae*–AgNPs

| | Langmuir | | | Freundlich | | |
|---|---|---|---|---|---|---|
| | $q_{max}$ | $K_L$ | $R^2$ | $K_F$ | $n$ | $R^2$ |
| *S. cerevisiae* | 17.12 | 0.1890 | 0.9893 | 4.559 | 2.990 | 0.8117 |
| *S. cerevisiae*–AgNPs | 15.01 | 0.1802 | 0.9934 | 3.933 | 3.013 | 0.8433 |

Langmuir model: $C_e/q_e = 1/q_{max}K_L + C_e/q_{max}$, where $C_e$ (mg $L^{-1}$) and $q_e$ (mg $g^{-1}$) represent the equilibrium concentration of $Cd^{2+}$ and the adsorption capacity, respectively. The $q_{max}$ (mg $g^{-1}$) and $K_L$ (L $mg^{-1}$) represent the maximum adsorption capacity and the Langmuir adsorption constant, respectively. Freundlich model: $q_e = K_F C_e^{1/n}$, where $C_e$ (mg $L^{-1}$) and $q_e$ (mg $g^{-1}$) represent $Cd^{2+}$ equilibrium concentration and the amount of adsorbed $Cd^{2+}$ at equilibrium, respectively. The constant of $K_F$ and n represents the uptake capacity and adsorption intensity, respectively

2011). There was a little difference on adsorption capacity between *S. cerevisiae* and *S. cerevisiae*–AgNPs (Table 2). The $Cd^{2+}$ adsorption capacity of *S. cerevisiae*–AgNPs was weakened, because adsorption sites of *S. cerevisiae* surface were occupied by AgNPs. The chief compositions and structure of *S. cerevisiae*–AgNPs were not altered. The functional groups still exist on *S. cerevisiae* surface, which would help *S. cerevisiae*–AgNPs to adsorb heavy metal. *S. cerevisiae*–AgNPs retained the ability of heavy metal removal.

## Application of *S. cerevisiae*–AgNPs on simulated wastewater

In order to improve the applications of this method in water treatment, adsorption experiments for various heavy metals were performed (Table 3). The removal efficiency for $Pb^{2+}$, $Cu^{2+}$, $Hg^{2+}$, $Zn^{2+}$, $Mn^{2+}$, $Ni^{2+}$, $Cr^{6+}$ and $As^{5+}$ was 91.75, 43.58, 19.72, 22.56, 22.53, 12.47, 6.25 and 9.65%, respectively. High removal efficiency for $Pb^{2+}$ was achieved due to $Pb^{2+}$ as soft ion (Chen and Wang 2010). Low removal efficiency for $Cr^{6+}$ or $As^{5+}$ could be relevant

**Table 3** Removal percentage of different kinds of heavy metals by *S. cerevisiae*–AgNPs

| The removal percentage of heavy metals (%) | | | | | | | |
|---|---|---|---|---|---|---|---|
| Cr | As | Pb | Cu | Mn | Zn | Hg | Ni |
| 6.25 | 9.65 | 91.75 | 43.58 | 22.53 | 22.56 | 19.72 | 12.47 |

to electrostatic repulsion between the negatively charged $Cr_2O_7^{2-}$ or $AsO_4^{3-}$ and the negatively charged *S. cerevisiae*–AgNPs. The simulated wastewater containing *E. coli*, $Cd^{2+}$ and $Pb^{2+}$ was treated using *S. cerevisiae*–AgNPs (Table 4). After 30-min reaction, *E. coli* cannot be detected; the removal efficiency for $Pb^{2+}$ reached 90.56%, for $Cd^{2+}$ reached 78%. The results showed that *S. cerevisiae*–AgNPs could be used to treat practical wastewater. Various adsorbents including inorganic nanomaterials, organic biomaterials for the removal of heavy metal or bacteria from aqueous systems were studied (Table S1). Although it is not always possible to make direct

**Table 4** Concentration changes of *E. coli*, Cd and Pb in the simulated contaminated water using *S. cerevisiae*–AgNPs

| Incubation time (min) | Cd (mg $L^{-1}$) | Pb (mg $L^{-1}$) | *E. coli* (CFU $mL^{-1}$) |
|---|---|---|---|
| 0 | 10.0 | 10.0 | $\approx 4.71 \times 10^7$ |
| 30 | 2.20 | 0.944 | Not detectable |
| 60 | 2.45 | 0.951 | Not detectable |
| 120 | 2.45 | 1.086 | Not detectable |

comparisons between different adsorbents in terms of pollutants removal from water, these adsorbents obviously cannot be used to remove both heavy metal and bacteria. *S. cerevisiae*–AgNPs possess the ability of removing both heavy metal and bacteria.

## Conclusion

A simple, rapid, environmentally friendly method for *S. cerevisiae*–AgNPs synthesis was developed to remove pollutants from water. This method can avoid high cost, complicated synthesis process and environmentally unfriendly chemistry reagent. More importantly, the antibacterial *S. cerevisiae*–AgNPs have good capacity of removing heavy metal. The present method will provide new insight into water treatment by bionanocomposites.

**Acknowledgements** This work was supported by the National Natural Science Foundation of China (51408214, 31671635, 31400374, 41501343), the Scientific Research Foundation of Hunan Provincial Education Department (14B066), China Postdoctoral Science Foundation (2014M552129), the Open Foundation of Chemo/Biosensing and Chemometrics State Key Laboratory (2014018).

## References

Ahmad B, Shireen F, Bashir S, Khan I, Azam S (2016) Green synthesis, characterisation and biological evaluation of AgNPs using *Agave americana*, *Mentha spicata* and *Mangifera indica* aqueous leaves extract. IET Nanobiotechnol 10:281–287. doi:10.1049/iet-nbt.2015.0053

Ali I (2010) The quest for active carbon adsorbent substitutes: inexpensive adsorbents for toxic metal ions removal from wastewater. Sep Purif Rev 39:95–171. doi:10.1080/15422119.2010.527802

Ali I (2012) New generation adsorbents for water treatment. Chem Rev 112(10):5073–5091. doi:10.1021/cr300133d

Ali I (2014) Water treatment by adsorption columns: evaluation at ground level. Sep Purif Rev 43:175–205. doi:10.1080/15422119.2012.748671

Ali I, Gupta VK (2007) Advances in water treatment by adsorption technology. Nat Protoc 1:2661–2667. doi:10.1038/nprot.2006.370

Ali I, Asim M, Khan TA (2012) Low cost adsorbents for the removal of organic pollutants from wastewater. J Environ Manag 113:170–183. doi:10.1016/j.jenvman.2012.08.028

Ali I, Al-Othman ZA, Alwarthan A (2016a) Synthesis of composite iron nano adsorbent and removal of ibuprofen drug residue from water. J Mol Liq 219:858–864. doi:10.1016/j.molliq.2016.04.031

Ali I, Al-Othman ZA, Alharbi OML (2016b) Uptake of pantoprazole drug residue from water using novel synthesized composite iron nano adsorbent. J Mol Liq 218:465–472. doi:10.1016/j.molliq.2016.02.088

Ali I, al-Othman ZA, Al-Warthan A (2016c) Sorption, kinetics and thermodynamics studies of atrazine herbicide removal from water using iron nano-composite material. Int J Environ Sci Technol 13:733–742. doi:10.1007/s13762-015-0919-6

Barboza NR, Amorim SS, Santos PA, Reis FD, Cordeiro MM, Guerra-Sá R, Leão VA (2015) Indirect manganese removal by *Stenotrophomonas* sp. and *Lysinibacillus* sp. isolated from brazilian mine water. Biomed Res. doi:10.1155/2015/925972

Belala Z, Jeguirim M, Belhachemi M, Addoun F, Trouve G (2011) Biosorption of copper from aqueous solutions by date stones and palm-trees waste. Environ Chem Lett 9:65–69. doi:10.1007/s10311-009-0247-5

Chen C, Wang JL (2010) Removal of heavy metal ions by waste biomass of Saccharomyces cerevisiae. J Environ Eng 136:95–102. doi:10.1061/(ASCE)EE.1943-7870.0000128

Chen C, Wen D, Wang J (2014) Cellular surface characteristics of *Saccharomyces cerevisiae* before and after Ag(I) biosorption. Bioresour Technol 156:380–383. doi:10.1016/j.biortech.2014.01.065

Clares ME, Guerrero MG, García-González M (2015) Cadmium removal by *Anabaena* sp. ATCC 33047 immobilized in polyurethane foam. Int J Environ Sci Technol 12:1793–1798. doi:10.1007/s13762-014-0743-4

Das SK, Khan MM, Guha AK, Das AR, Mandal AB (2012) Silver-nano biohybride material: synthesis, characterization and application in water purification. Bioresour Technol 24:495–499. doi:10.1016/j.biortech.2012.08.071

Das SK, Khan MM, Parandhaman T, Laffir F, Guha AK, Sekaran G (2013) Nano-silica fabricated with silver nanoparticles: antifouling adsorbent for efficient dye removal, effective water disinfection and biofouling control. Nanoscale 5(12):5549–5560. doi:10.1039/c3nr00856h

Fawell J, Nieuwenhuijsen MJ (2003) Contaminants in drinking water. Br Med Bull 68:199–208. doi:10.1093/bmb/ldg027

Hansda A, Kumar V, Anshumali (2016) A comparative review towards potential of microbial cells for heavy metal removal with emphasis on biosorption and bioaccumulation. World J Microbiol Biotechnol 32:170. doi:10.1007/s11274-016-2117-1

Javanbakht V, Alavi SA, Zilouei H (2014) Mechanisms of heavy metal removal using microorganisms as biosorbent. Water Sci Technol 69:1775–1787. doi:10.2166/wst.2013.718

Korbekandi H, Mohseni S, Mardani Jouneghani R, Pourhossein M, Iravani S (2016) Biosynthesis of silver nanoparticles using Saccharomyces cerevisiae. Artif Cells Nanomed Biotechnol 44(1):235–239. doi:10.3109/21691401.2014.937870

Li PS, Tao HC (2015) Cell surface engineering of microorganisms towards adsorption of heavy metals. Crit Rev Microbiol 41:140–149. doi:10.3109/1040841X.2013.813898

Li C, Xu Y, Jiang W, Dong X, Wang D, Liu B (2013) Effect of NaCl on the heavy metal tolerance and bioaccumulation of *Zygosaccharomyces rouxii* and *Saccharomyces cerevisiae*. Bioresour Technol 143:46–52. doi:10.1016/j.biortech

Lin S, Huang R, Cheng Y, Liu J, Lau BL, Wiesner MR (2013) Silver nanoparticle-alginate composite beads for point-of-use drinking water disinfection. Water Res 47:3959–3965. doi:10.1016/j.watres.2012.09.005

Loo SL, Fane AG, Lim TT, Krantz WB, Liang YN, Liu X, Hu X (2013) Superabsorbent cryogels decorated with silver nanoparticles as a novel water technology for point-of-use disinfection. Environ Sci Technol 47:9363–9371. doi:10.1021/es401219s

Nam KT, Lee YJ, Krauland EM, Kottmann ST, Belcher AM (2008) Peptide-mediated reduction of silver ions on engineered biological scaffolds. ACS Nano 2(7):1480–1486. doi:10.1021/nn800018n

Nancharaiah YV, Venkata Mohan S, Lens PN (2015) Metals removal and recovery in bioelectrochemical systems: a review. Bioresour Technol 195:102–114. doi:10.1016/j.biortech

Naumann D (2006) Encyclopedia of analytical chemistry. Wiley, Hoboken, pp 1–29

Park TJ, Lee KG, Lee SY (2016) Advances in microbial biosynthesis of metal nanoparticles. Appl Microbiol Biotechnol 100(2):521–534. doi:10.1007/s00253-015-6904-7

Salunke BK, Sawant SS, Lee SI, Kim BS (2016) Microorganisms as efficient biosystem for the synthesis of metal nanoparticles: current scenario and future possibilities. World J Microbiol Biotechnol 32:88. doi:10.1007/s11274-016-2044-1

Salunkhe RB, Patil SV, Salunke BK, Patil CD, Sonawane AM (2011) Studies on silver accumulation and nanoparticle synthesis by *Cochliobolus lunatus*. Appl Biochem Biotechnol 165(1):221–234. doi:10.1007/s12010-011-9245-8

Selvakumar R, Jothi NA, Jayavignesh V, Karthikaiselvi K, Antony GI, Sharmila PR (2011) As(V) removal using carbonized yeast cells containing silver nanoparticles. Water Res 45(2):583–592. doi:10.1016/j.watres.2010.09.034

Sreeprasad TS, Maliyekkal MS, Deepti K, Chaudhari K, Xavier PL, Pradeep T (2011) Transparent, luminescent, antibacterial and patternable film forming composites of graphene oxide/reduced graphene oxide. ACS Appl Mater Interfaces 3:2643–2654. doi:10.1021/am200447p

Velusamy P, Kumar GV, Jeyanthi V, Das J, Pachaiappan R (2016) Bio-inspired green nanoparticles: synthesis, mechanism, and antibacterial application. Toxicol Res 32:95–102. doi:10.5487/TR.2016.32.2.095

Wang J, Chen C (2006) Biosorption of heavy metals by *Saccharomyces cerevisiae*: a review. Biotechnol Adv 24(5):427–451. doi:10.1016/j.biotechadv.2006.03.001

Wang H, Liu J, Wu X, Tong Z, Deng Z (2013) Tailor-made Au@Ag core–shell nanoparticle 2D arrays on protein-coated graphene oxide with assembly enhanced antibacterial activity. Nanotechnology 24:205102. doi:10.1088/0957-4484/24/20/205102

Wei X, Luo M, Li W, Yang L, Liang X, Xu L, Kong P (2012) Synthesis of silver nanoparticles by solar irradiation of cell-free *Bacillus amyloliquefaciens* extracts and $AgNO_3$. Bioresour Technol 103(1):273–278. doi:10.1016/j.biortech.2011.09.118

Yin Y, Liu J, Jiang G (2012) Sunlight-induced reduction of ionic Ag and Au to metallic nanoparticles by dissolved organic matter. ACS Nano 6:7910–7919. doi:10.1021/nn302293r

Zhang XF, Liu ZG, Shen W, Gurunathan S (2016) Silver nanoparticles: synthesis, characterization, properties, applications, and therapeutic approaches. Int J Mol Sci 17:1534. doi:10.3390/ijms17091534